Electronic Supplementary Information (ESI)

Experimental

***Materials Synthesis*:** The α-Fe_2O_3 MSHSs hollow microspheres were prepared by a spray drying method followed by annealing in air. In a typical synthesis (Sample 1, see Table S1), $Fe(NO_3)_3 \cdot 9H_2O$ (10 mmol) and sucrose (10 mmol) were dissolved in H_2O (100 mL) to form a clear solution. The resulting solution was then spray dried using a Buchi mini spray drier B-290 at an inlet temperature of 220 ºC, an aspirator rate of 100 %, a rotameter setting of 60 mm, and a pump rate of 5 % (1.5 mL/min). Nitrogen was used as the drying gas. These settings resulted in an outlet temperature of ~ 130 ºC. The spray dried samples (iron nitrate-sucrose composite) were then annealed in air at 400 ºC for 5 hours with a temperature ramp rate of 2 ºC/min. To study the influence of synthesis parameters on the structures, a series of samples were prepared by adjusting the feeding ratio of reagents, the temperature ramp rate, and the choices of organic matrices. The detailed synthesis conditions for all samples are listed in Table S1.

***Characterization*:** XRD patterns were collected on a German Bruker D8 Advanced X-Ray Diffractometer with Ni filtered Cu Kα radiation (40 kV, 30 mA). Field emission SEM images were obtained on a JEOL JSM 7800 with accelerating voltages of 5.0 and 15.0 kV, respectively, while TEM images were taken on Philips Tecnai F20 (operated at 200 kV). Thermo gravimetric analysis (TGA) was carried out on a TGA/DSC1 STAR^e System under air flow (25 − 1000 ºC, 5 ºC/min). Nitrogen adsorption isotherms were measured at 77 K using a TriStar II Surface Area and Porosity analyser (Micromeritics). The samples were degassed under vacuum for 6 hours at 200 ºC before analysis. BET surface area was calculated from the adsorption branch in relative pressure (p/p_0) range of 0.05 − 0.30.

***Electrochemical Measurement*:** The electrochemical measurements were carried out in homemade two-electrode Swagelok type cells. The working electrode is consisted of active material, conductive acetylene black, and polyvinylidene fluoride binder in a weight ratio of 70:20:10. Lithium chips were used as both the counter electrode and reference electrode. 1 M $LiPF_6$ in a mixture of ethylene carbonate, dimethyl carbonate, and diethyl carbonate (1:1:1 in volume) was used as the electrolyte. Cell assembly was carried out in an Ar-filled glovebox with moisture and oxygen concentrations below 1.0 ppm. CV measurements were performed on a Solartron 1480 MultiStat instrument. The galvanostatic charge-discharge tests were performed on a MTI 8 Channels Battery Analyzer.

Table 1. Synthesis conditions for α-Fe_2O_3 hollow structures/nanostructures.

Sample Name	Organic Species	Iron Nitrate	Temperature ramp rate
Sample 1	Sucrose, 10 mmol	10 mmol	2 ºC/min
Sample 2	Sucrose, 7.5 mmol	10 mmol	2 ºC/min
Sample 3	Sucrose, 15 mmol	10 mmol	2 ºC/min
Sample 4	Sucrose, 20 mmol	10 mmol	2 ºC/min
Sample 5	Sucrose, 10 mmol	10 mmol	0.5 ºC/min
Sample 6	Sucrose, 10 mmol	10 mmol	5 ºC/min
Sample 7	Glucose, 20 mmol	10 mmol	2 ºC/min
Sample 8	PVA,[a] 4 g	10 mmol	2 ºC/min

a PVA: polyvinyl alcohol

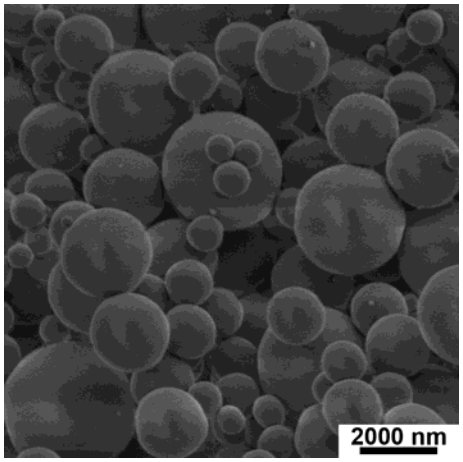

Figure S1. FESEM images of iron nitrate-sucrose composite microspheres (sucrose/iron nitrate ratio: 10/10).

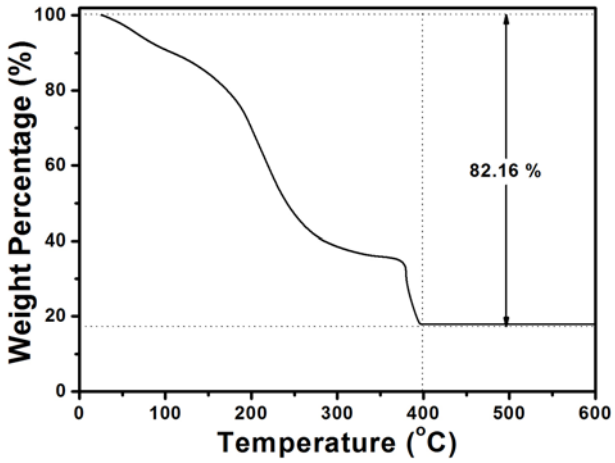

Figure S2. TGA curve of the iron nitrate-sucrose composites (sucrose/iron nitrate ratio: 10/10).

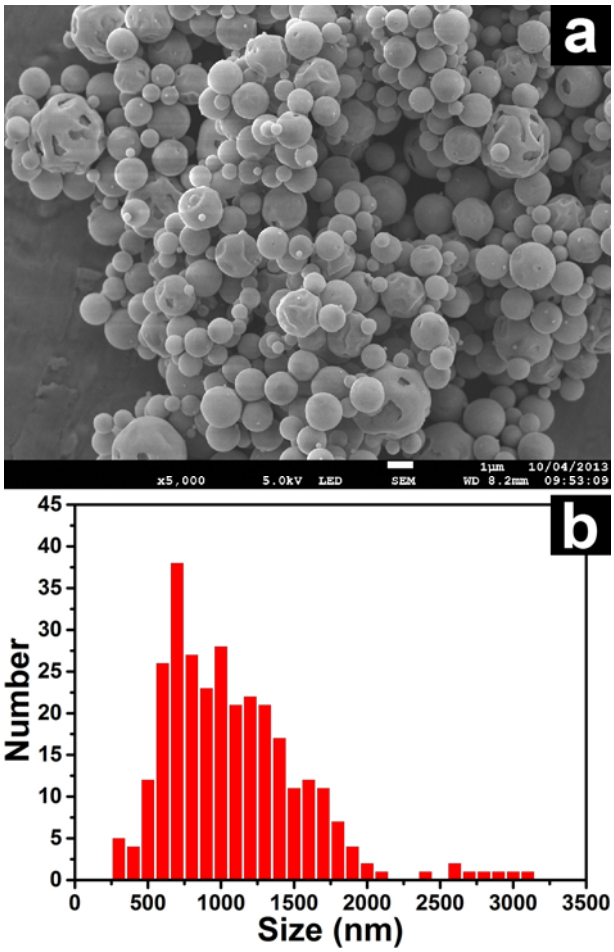

Figure S3. Low-magnification SEM image and the corresponding particle size distribution of α-Fe_2O_3 MSHSs.

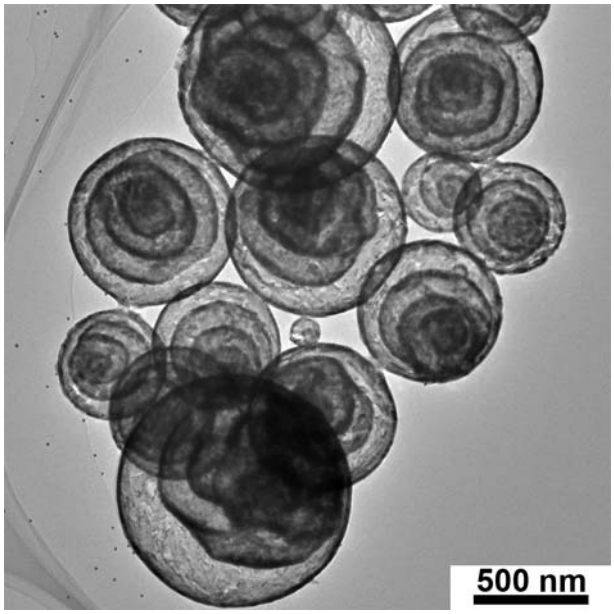

Figure S4. Low-magnification TEM image of α-Fe_2O_3 MSHSs.

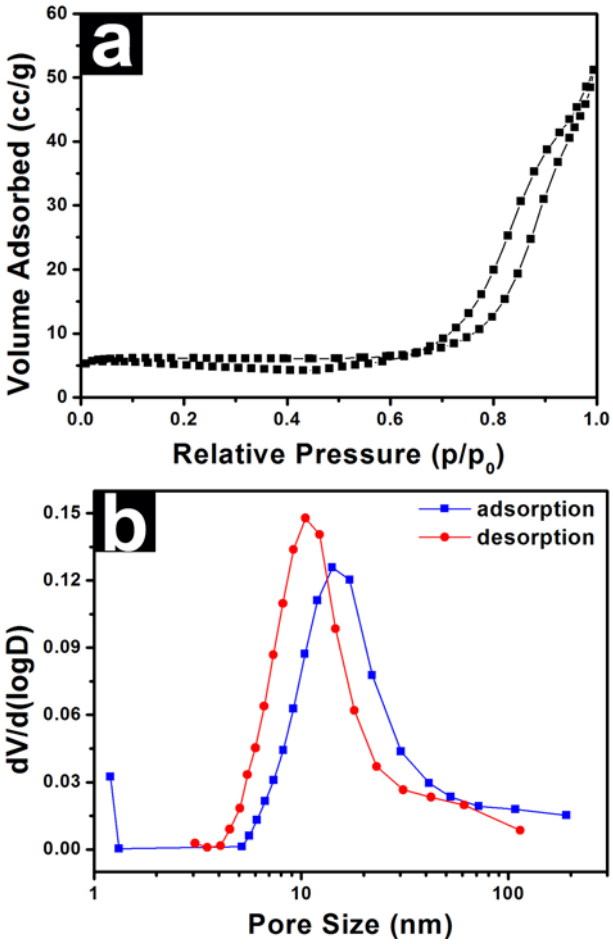

Figure S5. Nitrogen adsorption isotherm (a) and pore size distributions (b) of the α-Fe_2O_3 MSHSs (Sample 1).

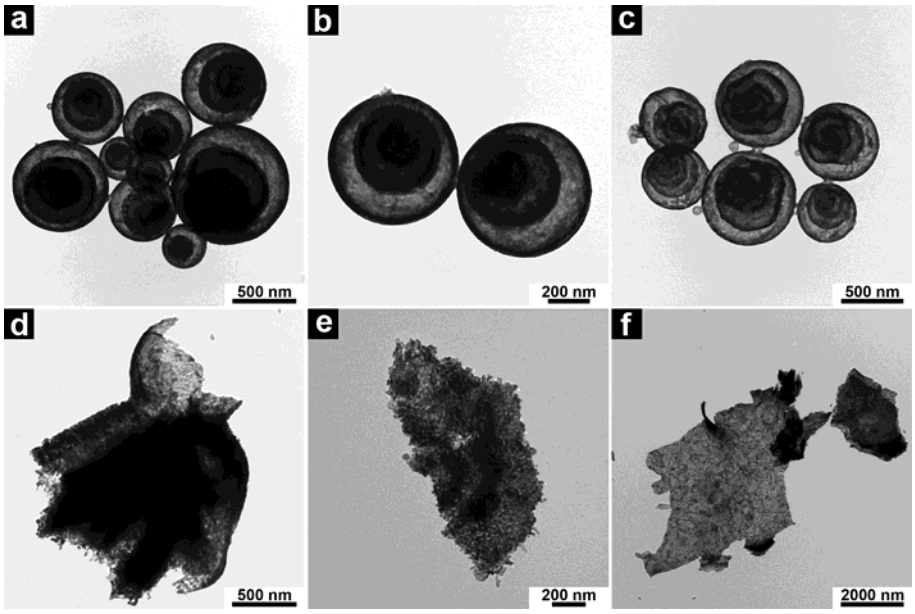

Figure S6. TEM images of Sample 2 (a and b, sucrose/iron nitrate ratio: 7.5/10), Sample 1 (c, sucrose/iron nitrate ratio: 10/10), Sample 3 (d and e, sucrose/iron nitrate ratio: 15/10), and Sample 4 (f, sucrose/iron nitrate: 20/10).

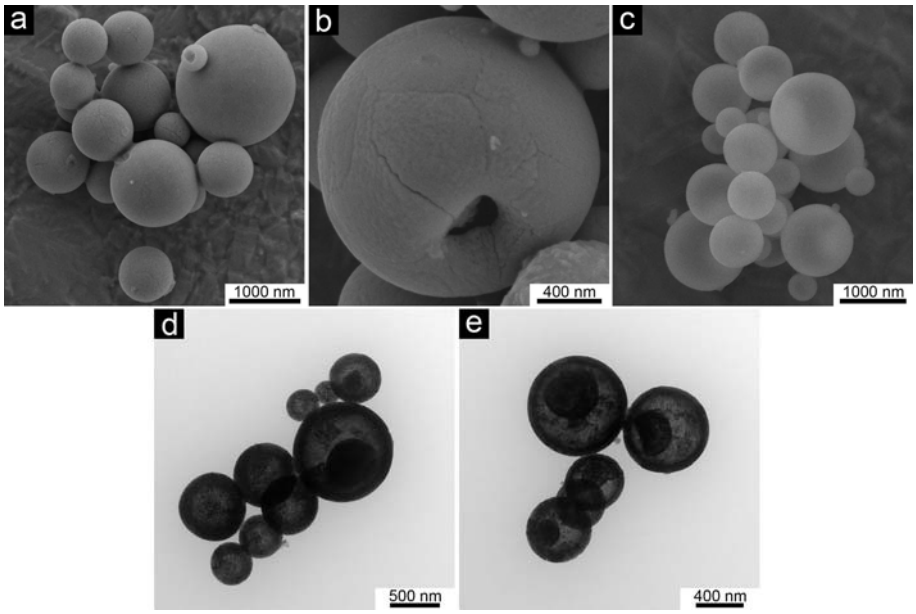

Figure S7. FESEM (a − c) and TEM (d, e) images of α-Fe_2O_3 hollow structures (Sample 5, temperate ramp rate: 0.5 ºC/min). For a and b, the accelerating voltage is 5 kV; for c, the accelerating voltage is 15 kV.

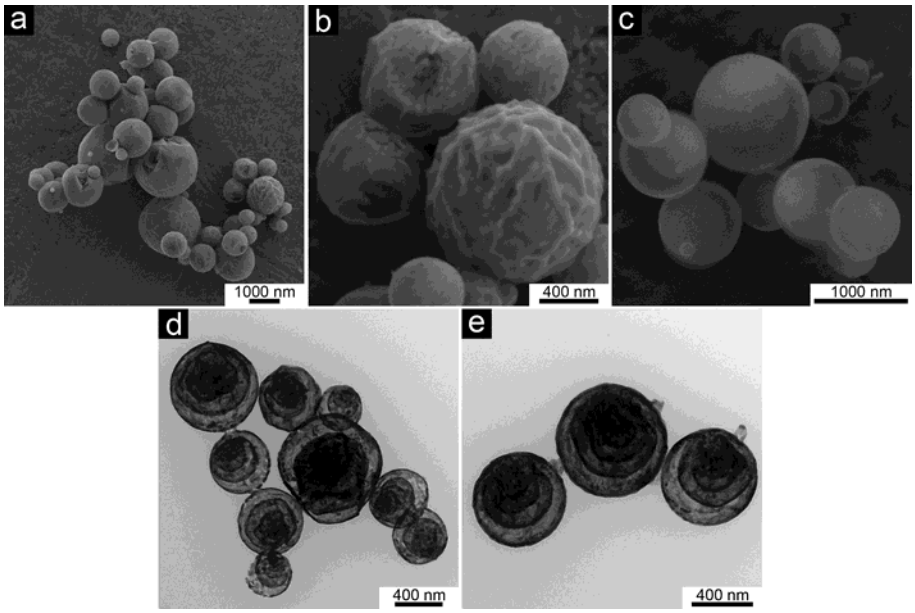

Figure S8. FESEM (a − c) and TEM (d, e) images of α-Fe_2O_3 hollow structures (Sample 6, temperature ramp rate: 5 ºC/min). For a and b, the accelerating voltage is 5 kV; for c, the accelerating voltage is 15 kV.

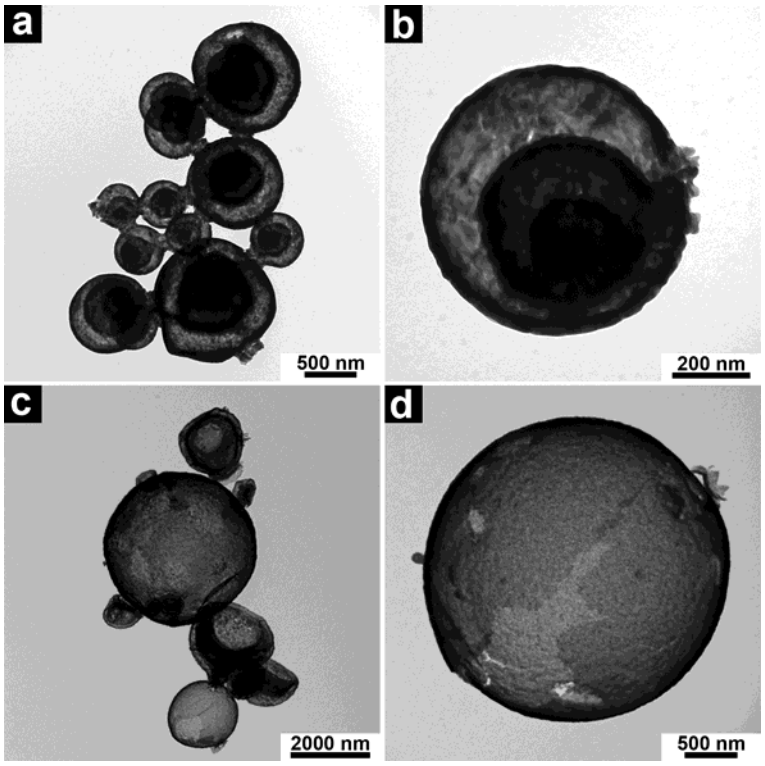

Figure S9. TEM images of α-Fe_2O_3 hollow structures using glucose (a and b, Sample 7) and PVA (c and d, Sample 8) as the organic species.

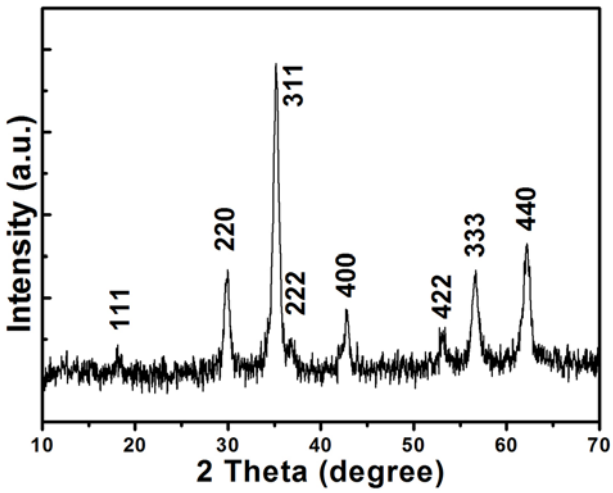

Figure S10. XRD pattern of the $ZnFe_2O_4$ yolk-shell structures.

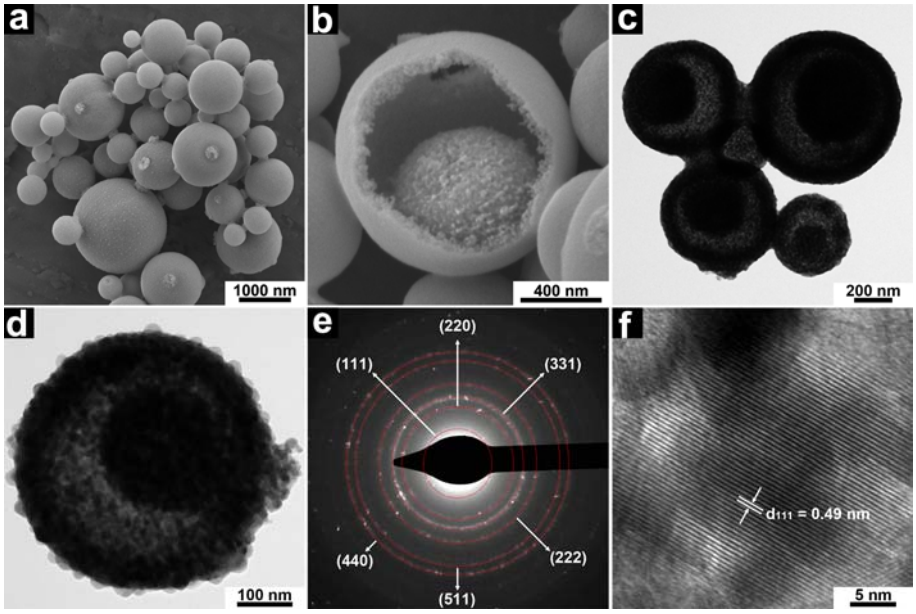

Figure S11. FESEM (a, b), TEM (c, d), SAED (e) and HRTEM (f) images of $ZnFe_2O_4$ yolk-shell structures.

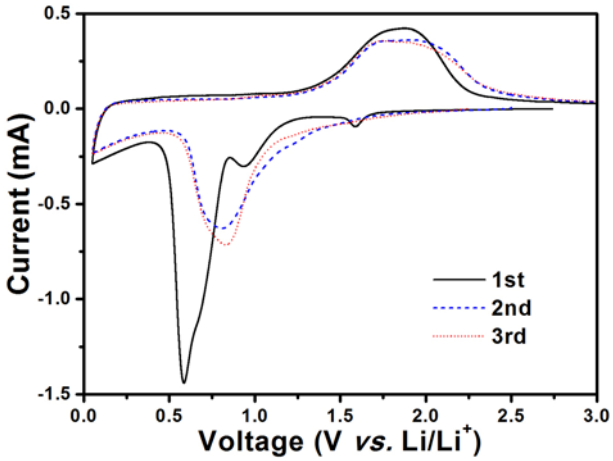

Figure S12. CVs of α-Fe_2O_3 MSHSs for the initial three cycles at a rate of 0.1 mA s^{-1}.

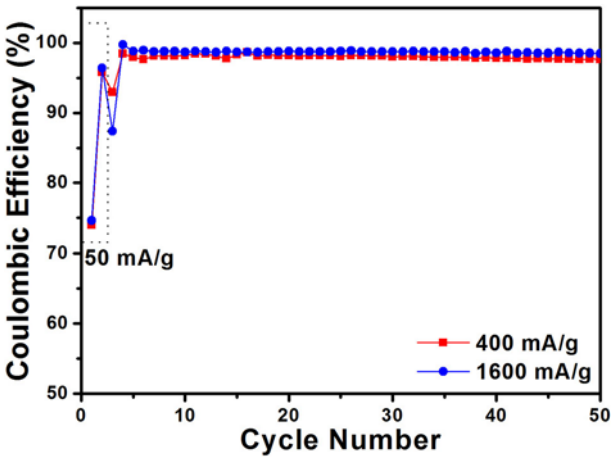

Figure S13. Coulombic efficiency *vs.* cycle number.

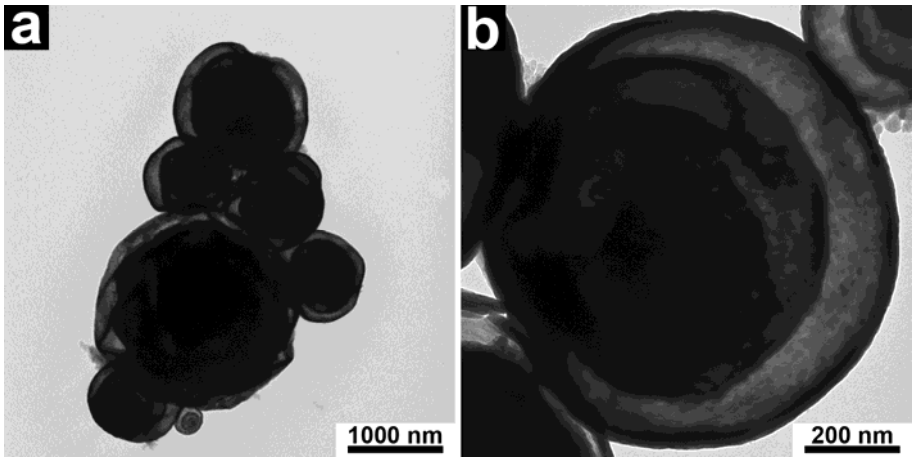

Figure S14. TEM images of the α-Fe_2O_3 MSHSs after the first discharge-charge cycle at 400 mA g^{-1}.

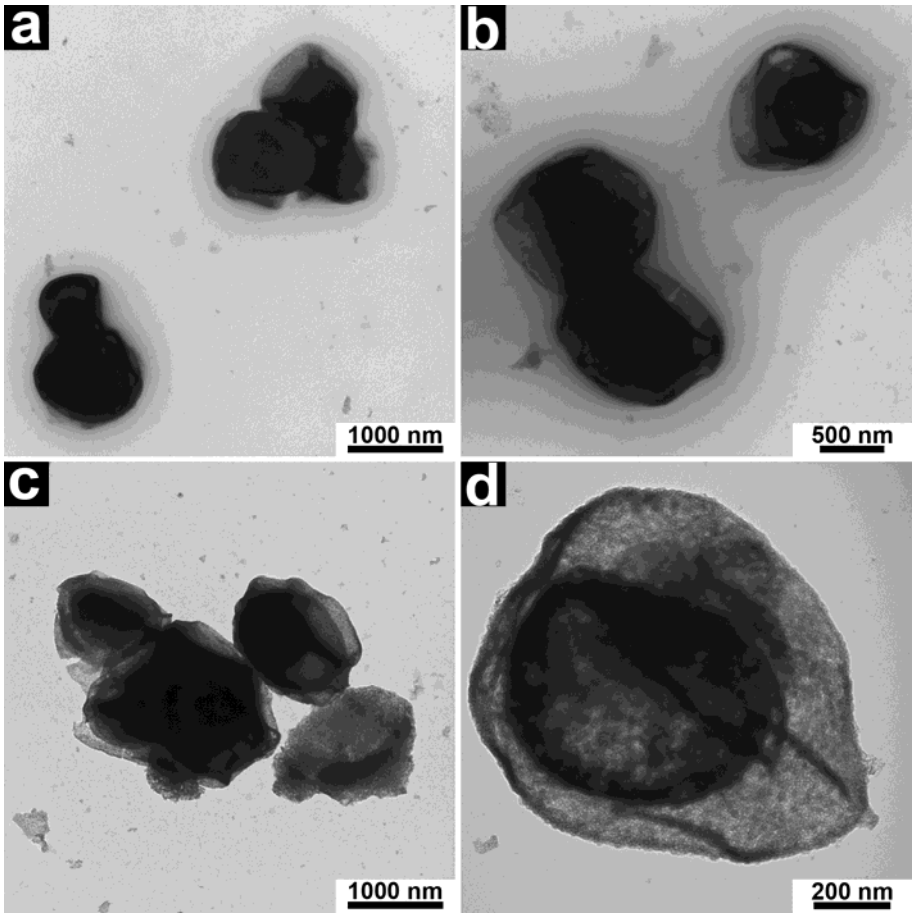

Figure S15. TEM images of the α-Fe_2O_3 MSHSs after 50 discharge-charge cycles at 400 mA g^{-1}.